# Magnetospheric Multiscale Satellites Observations of Parallel Electric Fields Associated with Magnetic Reconnection

R. E. Ergun,[1,2] K. A. Goodrich,[1,2] F. D. Wilder,[2] J. C. Holmes,[1,2] J. E. Stawarz,[1,2] S. Eriksson,[2] A. P. Sturner,[1,2] D. M. Malaspina,[1] M. E. Usanova,[1] R. B. Torbert,[3,4] P.-A. Lindqvist,[5] Y. Khotyaintsev,[6] J. L. Burch,[4] R. J. Strangeway,[7] C. T. Russell,[7] C. J. Pollock,[8] B. L. Giles,[8] M. Hesse,[8] L. J. Chen,[9] G. Lapenta,[10] M. V. Goldman,[11] D. L. Newman,[11] S. J. Schwartz,[2,12] J. P. Eastwood,[12] T. D. Phan,[13] F. S. Mozer,[13] J. Drake,[9] M. A. Shay,[14] P. A. Cassak,[15] R. Nakamura,[16] and G. Marklund[5]

[1]*Department of Astrophysical and Planetary Sciences, University of Colorado, Boulder, Colorado 80303, USA*
[2]*Laboratory of Atmospheric and Space Sciences, University of Colorado, Boulder, Colorado 80303, USA*
[3]*University of New Hampshire, Durham, New Hampshire 03824, USA*
[4]*Southwest Research Institute, San Antonio, Texas 78238, USA*
[5]*KTH Royal Institute of Technology, Stockholm, Sweden*
[6]*Swedish Institute of Space Physics (Uppsala), Uppsala, Sweden*
[7]*University of California, Los Angeles, Los Angeles, California 90095, USA*
[8]*NASA, Goddard Space Flight Center, Greenbelt, Maryland 20771, USA*
[9]*University of Maryland, College Park, Maryland 20742, USA*
[10]*Leuven Universiteit, Leuven, Belgium*
[11]*Department of Physics, University of Colorado, Boulder, Colorado 80303, USA*
[12]*The Blackett Laboratory, Imperial College London, United Kingdom*
[13]*Space Sciences Laboratory, University of California, Berkeley, California 94720, USA*
[14]*University of Delaware, Newark, Delaware 19716, USA*
[15]*West Virginia University, Morgantown, West Virginia 26506, USA*
[16]*Space Research Institute, Austrian Academy of Sciences, Graz, Austria*

We report observations from the Magnetospheric Multiscale satellites of parallel electric fields ($E_\parallel$) associated with magnetic reconnection in the subsolar region of the Earth's magnetopause. $E_\parallel$ events near the electron diffusion region have amplitudes on the order of 100 mV/m, which are significantly larger than those predicted for an antiparallel reconnection electric field. This Letter addresses specific types of $E_\parallel$ events, which appear as large-amplitude, near unipolar spikes that are associated with tangled, reconnected magnetic fields. These $E_\parallel$ events are primarily in or near a current layer near the separatrix and are interpreted to be double layers that may be responsible for secondary reconnection in tangled magnetic fields or flux ropes. These results are telling of the three-dimensional nature of magnetopause reconnection and indicate that magnetopause reconnection may be often patchy and/or drive turbulence along the separatrix that results in flux ropes and/or tangled magnetic fields.

*Introduction.*—Magnetic reconnection is a fundamental process that enables a change of magnetic topology in space, solar, astrophysical, and laboratory plasmas. While understood on ion scales in two dimensions, the electron-scale physics and the three-dimensional nature of magnetic reconnection is currently a topic of active investigation. The Magnetospheric Multiscale (MMS) mission, which has four spacecraft in a close tetrahedron, is designed to study the three-dimensional structure of magnetic reconnection focusing on the electron diffusion region (EDR) [1,2]. MMS has two phases, the first of which examines reconnection near the subsolar magnetopause. This region has been observed extensively at the ion scale [3–9], but little is known at electron skin depth ($\lambda_e$) scales. This region has also been examined extensively with numerical simulations and analytic analysis [10–22].

In the subsolar magnetopause, the shocked solar wind plasma, called magnetosheath plasma, impinges on and reconnects with the Earth's magnetosphere. The magnetosphere plasma differs from the magnetosheath plasma in density ($n$), ion and electron temperatures ($T_i$ and $T_e$), and magnetic field ($\boldsymbol{B}$) strength. The two sides of the reconnection region therefore have dissimilar Alfvén speeds, which influence reconnection rates [19]. As a result, magnetic reconnection at the Earth's magnetopause is expected to be asymmetric [18–20].

In the magnetosheath plasma, $n$ is a few tens of $cm^{-3}$ and $T_e$ is most often between 50 and 200 eV. $T_i$ is typically several times $T_e$. The Earth's magnetosphere is dominated by magnetic ($\boldsymbol{B}$) pressure ($|\boldsymbol{B}| \sim 50$ nT). Often, $n$ is a few $cm^{-3}$ or less. $T_e$ and $T_i$ are on the order of 1 keV. One noteworthy exception is the intermittent presence of cold

($<10$ eV, $n \sim 1$ cm$^{-3}$) plasma in the magnetosphere. When present, the mixing with the magnetosheath plasma can result in intense wave emissions (e.g., [23]).

Numerical simulations have explained many of the observed large-scale features of magnetopause reconnection in two dimensions and predict several of the electron-scale features [12,13,18–20,24]. The three-dimensional topology of magnetic reconnection is not as well understood; reconnection can drive turbulence, which can lead to complex magnetic topologies, e.g., [25,26]. In addition, turbulence in the magnetosheath plasma can introduce irregular boundary conditions, which also can result in complex magnetic topologies. For example, three-dimensional magnetic reconnection can be patchy, that is, not lying on a continuous $X$ line and having multiple $X$ points or $X$ lines, e.g., [9].

The MMS satellites have successfully detected the EDR [27] and verified much of the fundamental electron physics predicted by simulation and theory, e.g., [21]. The observations also contain an abundance of new information on magnetic reconnection. This Letter concentrates on particular types of $E_\parallel$ events, large amplitude and unipolar, that are observed in conjunction with complex magnetic field structures. We hypothesize that these $E_\parallel$ events represent secondary reconnection [25]. Patchy reconnection or turbulence along the separatrix can result in flux ropes and tangled magnetic fields, which ultimately must resolve or untangle. We denote secondary reconnection as the process of resolving flux ropes or tangled field lines.

*Observations.*—Figure 1 displays 5 s of data near (within a few $\lambda_e$) an EDR by the MMS1 spacecraft. This event, in particular, an encounter with the electron diffusion region by MMS2, has been discussed in detail [27]. The mission and its instruments are described in several articles [1,2,28–32].

The top panels [(a) and (b)] display the ion and electron differential energy flux (color) as a function of energy (vertical axis) and time [32]. Panel (c) plots the parallel and perpendicular values of $T_i$ and $T_e$. The colors are labeled on the right side of the plot. Panel (d) plots the magnetic field ($B$) [28,31] at 128 samples/s in geocentric solar ecliptic (GSE) coordinates. $X$ is toward the Sun, $Z$ is normal to the ecliptic plane, and $Y$ completes the system. At the beginning of the plot, MMS1 is in Earth's magnetosphere as characterized by $\sim$1 keV ions and positive $B_z$. The electrons, however, appear to be a mixture of magnetosheath plasma and magnetosphere plasma, indicating that MMS1 is on a reconnected $B$. At the end of the plot, MMS1 is in the magnetopause boundary.

The next three panels (e.g., displaying $E_x$, $E_y$, and $E_z$, respectively) plot the electric field ($E$) in GSE coordinates with three separate techniques. The black lines are from the double probe electric field instrument [28–30] at 32 samples/s. During this period, the uncertainty in the $E_x$ and $E_y$ is $\sim$1 mV/m. The alternating (positive-negative)
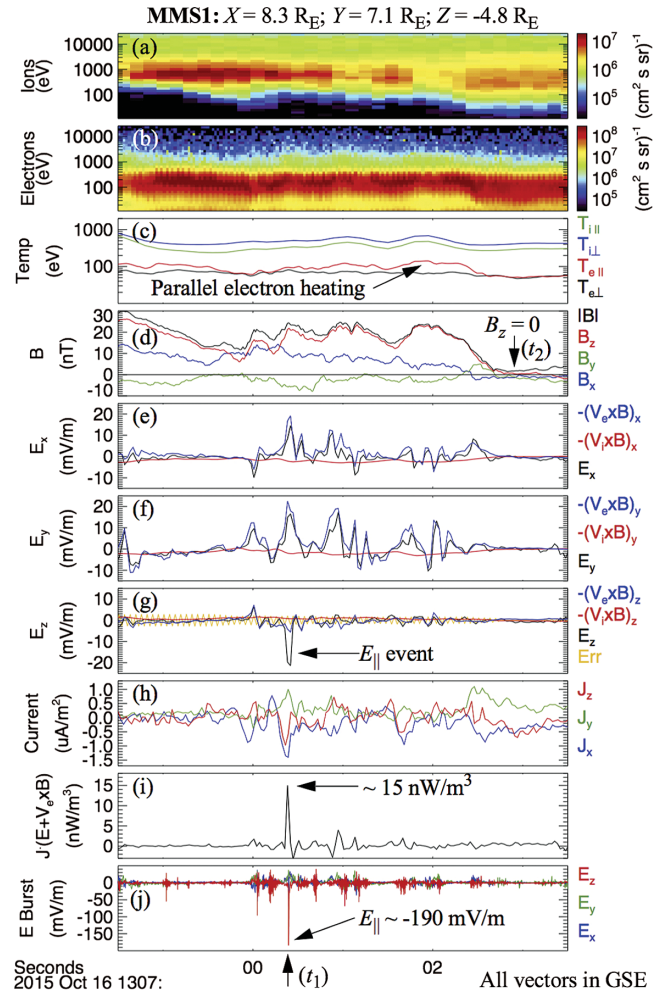


FIG. 1.   MMS1 near encounter with the EDR [27]. [(a) and (b)] The differential ion and electron energy flux as a function of energy (vertical axis) and time. (c) $T_i$ and $T_e$. (d) $B$. [(e)–(g)] Measured $E$ (black), $-V_i \times B$ (red), and $-V_e \times B$ (blue). The orange trace in (g) is the uncertainty in $E_z$, alternating positive and negative. (h) $J$ derived from $V_i - V_e$. (i) Energy dissipation $J \cdot (E + V_e \times B)$. (j) $E$ (from double probe) at 8192 samples/s.

orange trace in panel (g) represents the uncertainty in $E_z$ [29], which at the time is $\sim$3 mV/m. The blue lines ($-V_e \times B$) are derived from the cross product of the measured electron velocity ($V_e$, 32 samples/s) and $B$. The red lines ($-V_i \times B$) are derived from the measured ion velocity ($V_i$, 8 samples/s).

$E$ and ($-V_e \times B$) are in good agreement for most of the region whereas ($-V_i \times B$) clearly differs, suggesting that MMS1 is inside of an ion diffusion region or a Hall current region. Discrepancies between $E_y$ and ($-V_e \times B$)$_y$ can be attributed to uncertainty in $V_e$ in the $X$ direction due to spacecraft photoelectrons. The discrepancy between the measured $E_z$ and ($-V_e \times B$)$_z$ at 13:07:00.4 UT (which we call $t_1$), however, is clearly due to a parallel electric field, which, on a $\sim$30 ms time scale, reaches $\sim$$-20$ mV/m.
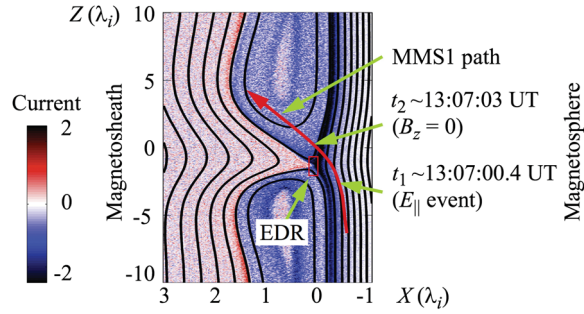
FIG. 2.   The approximate position of the MMS1 path (red line) inferred from observations and plotted over a simulation of asymmetric magnetic reconnection in the magnetopause (source: G. Lapenta). The $X$ axis is exaggerated relative to the $Z$ axis.

Panel (h) is the current derived as $\boldsymbol{J} = en(\boldsymbol{V}_i - \boldsymbol{V}_e)$ where $e$ is the fundamental charge. $J_z$ and $J_x$ spike to negative values immediately before the $E_\parallel$ event. $J_y$ has a positive value. The $E_\parallel$ spike begins [panel (g)] as $J_z$ reaches its negative peak. Both recover to near zero at the same time. Panel (i) displays $\boldsymbol{J} \cdot (\boldsymbol{E} + \boldsymbol{V}_e \times \boldsymbol{B})$, which represents dissipation in the electron frame.

Panel (j) displays $\boldsymbol{E}$ at 8192 samples/s (low-pass filtered ~3.3 kHz). The red trace is $E_z$, which is primarily parallel to $\boldsymbol{B}$ [Fig 1(d); $B_z \sim |\boldsymbol{B}|$]. One can see that $E_\parallel$ dominates the high-time resolution $\boldsymbol{E}$. These data resolve $E_\parallel$ at 13:07:00.4 UT as a unipolar signal reaching $\sim -190$ mV/m for a significantly shorter duration (~5 ms) than indicated in panel (g). This signal amplitude far exceeds the reconnection $\boldsymbol{E}$, which is expected to be between 1 and 5 mV/m, e.g., [21].

Figure (2) displays the approximate location of MMS1 with respect to a magnetopause reconnection region [27] during this event. There are several indications that MMS1 is less than several $\lambda_e$ ($\lambda_e \sim 2$ km) from the EDR. At $\sim 13\!:\!07\!:\!03$ UT (labeled $t_2$ in Figs. 1 and 2), $|\boldsymbol{B}|$ is near zero [Fig. 1(d)]. There is substantial electron heating as evidenced by $T_{e\parallel}$ [Fig. 1(c)] increasing over $T_{e\perp}$ prior to 13:07:03 UT. $\boldsymbol{V}_i$ is decoupled from $\boldsymbol{V}_e$ and $\boldsymbol{E}$ [Figs. 1(e)–(g)]. On a larger time scale, $\boldsymbol{V}_i$ reverses direction from $-Z$ to $+Z$ (not displayed; see [27]). MMS2, separated by 10 km, appears to have encountered the EDR [27].

In addition to the unipolar $E_\parallel$ event, strong fluctuations in $E_\parallel$ [Fig. 1(j)] are also observed near the EDR. These strong fluctuations appear as linear waves, frequently displaying nonlinear behavior. Such waves, believed to come from mixing of magnetosphere plasma with magnetosheath plasma, have been observed previously [23,33,34], and are discussed in a future article.

The large-amplitude, unipolar $E_\parallel$ event is clearly distinct and, to our knowledge, has not been previously reported. It is observed by MMS1 only. During the $E_\parallel$ event there are fluctuations in $\boldsymbol{B}$, in particular, in $|\boldsymbol{B}|$ and out of phase oscillations in $B_x$ and $B_y$ [Fig. 1(d)]. The $\boldsymbol{B}$ fluctuations suggest that a flux rope or a tangled magnetic field topology is associated with the magnetic reconnection process.
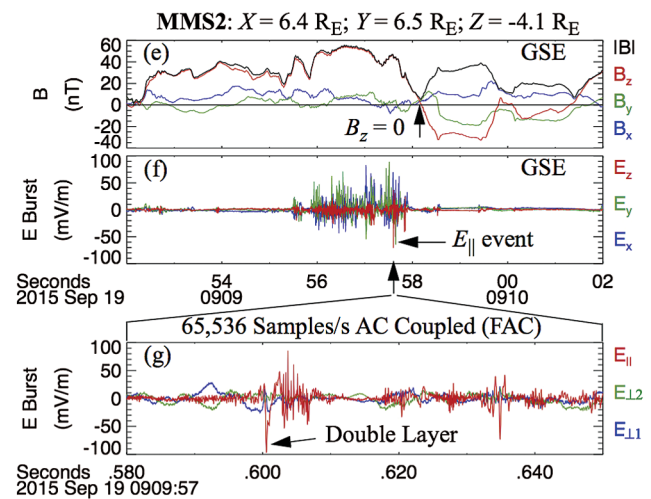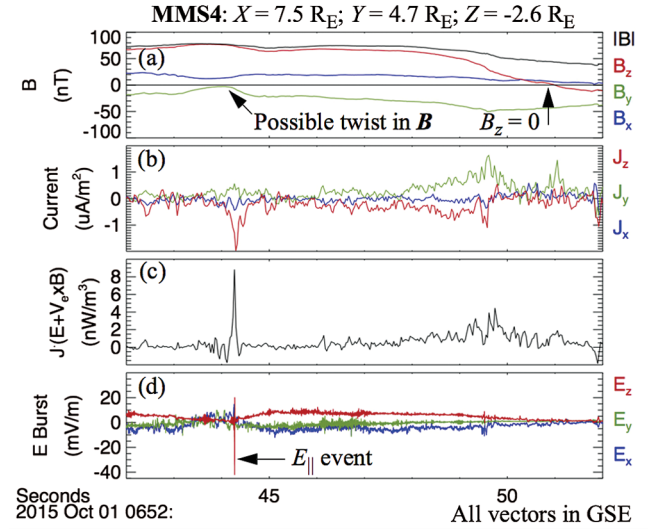


FIG. 3.   Near unipolar $E_\parallel$ events associated with fluctuating $\boldsymbol{B}$. [(a)–(d)] An event from October 1, 2015 06:52:44.2 UT observed by MMS4. The top panel displays $\boldsymbol{B}$. Panel (b) plots $\boldsymbol{J}$, panel (c) displays $\boldsymbol{J} \cdot (\boldsymbol{E} + \boldsymbol{V}_e \times \boldsymbol{B})$, and panel (d) plots $\boldsymbol{E}$ at 8192 samples/s. The $E_\parallel$ event is in the magnetosphere and ~7 s prior to a reversal in $B_z$. [(e)–(g)] Another strong, nearly unipolar $E_\parallel$ event. Again, the event appears with fluctuating $\boldsymbol{B}$, is in the magnetopause, is near to a null $|\boldsymbol{B}|$, and is near a reversal in $B_z$. This event was captured at 65536 samples/s [panel (g)], which is in field-aligned coordinates.

Larger-scale flux ropes have been observed [35,36] and simulated [25].

Several more isolated near unipolar, large-amplitude $E_\parallel$ events have been examined. Two such events are displayed in Fig. (3). These events have many common properties with the $E_\parallel$ event shown in Fig. (1). $\boldsymbol{V}_i$ is decoupled from $\boldsymbol{V}_e$ and $\boldsymbol{E}$. Parallel electron heating is observed. They occur near a reversal in $B_z$ and often a minimum in $|\boldsymbol{B}|$. $\boldsymbol{B}$ displays fluctuations. The first of these events has a clear peak in $\boldsymbol{J} \cdot (\boldsymbol{E} + \boldsymbol{V}_e \times \boldsymbol{B}) > 0$ indicating energy dissipation.

The $E_\parallel$ event [Fig. 3(d)] at 06:52:44.2 UT occurs in similar plasma conditions as the $E_\parallel$ event in Fig. (1).

The magnetic field [Fig. 3(a)] indicates a possible twist in the $B_x$ and $B_y$ components at the time of the $E_\parallel$ event. $J_z$ [Fig. 3(b)] has a negative excursion causing a peak in dissipation [Fig. 3(c)]. This event, however, may be farther away from the EDR than the event in Fig. 1.

The plots in Figs. 3(e) and 3(f) cover 10 s, during which (from 09:09:56 to 09:09:58 UT) intense wave emissions are measured in all components of **E**. Such emissions are frequent on the magnetosphere side of a null in $|\boldsymbol{B}|$ or a $B_z$ reversal (e.g., 23). The **E** signal is shown for a 70 ms period in Fig. 3(g). The $E_\parallel$ signal in Fig. 3(g) is ac coupled at $65,536$ samples/s [29]. At 09:09:57.60 a unipolar spike at $\sim -95$ mV/m (red trace) lasts for roughly 2 ms followed by parallel fluctuations that are often adjacent to double layers. The large fluctuations in the $E_x$ and $E_y$ greatly increase the uncertainty in $\boldsymbol{J} \cdot \boldsymbol{E}$ (not shown, measured at 30 ms cadence), so we cannot conclusively determine whether there is or is not strong dissipation in this particular event, especially given the short duration (2 ms) of $E_\parallel$.

*Discussion.*—The near unipolar $E_\parallel$ events in Figs. 1(j) and 3(d) differ from previous double layer observations [37–39] in that no strong fluctuations are adjacent to the $E_\parallel$ structure. Yet, the data indicate $\boldsymbol{J} \cdot \boldsymbol{E} > 0$, which suggests a double layer. Since $V_{ex}$ is >500 km/s (higher than the ion acoustic speed) in both of those events (not displayed), it is possible that the $E_\parallel$ structures pass by the spacecraft perpendicular to **B** rather than parallel to **B** (as often observed [37–39]); thus, strong fluctuations associated with accelerated electrons are not observed. It is also possible these $E_\parallel$ events are double layers that endure for short periods so that the measured signal represents the lifetime of the double layer.

The unipolar $E_\parallel$ event in Figs. 3(f) and 3(g) has similar characteristics to observations of double layers in the aurora (e.g., [37]) and plasma sheet [38] in that strong fluctuations are observed adjacent to the unipolar $E_\parallel$ structure. Double layers can develop from strong parallel currents [39] and often imply strong dissipation ($\boldsymbol{J} \cdot \boldsymbol{E} > 0$).

Several dozens of unipolar $E_\parallel$ events have been identified at the time of this Letter. All events are accompanied by fluctuations in **B**. Since MMS high-resolution data are selected at possible EDR regions, we do not suggest that the occurrence of such $E_\parallel$ events is limited to near an EDR. On the other hand, strong wave activity near the EDR often obscures identification and makes determination of $\boldsymbol{J} \cdot \boldsymbol{E} > 0$ difficult [e.g., Figs. 3(e) and 3(f)]. In addition, the MMS satellites are likely to detect only a small fraction of the $E_\parallel$ structures due to their small physical size. For this Letter, we concentrate on $E_\parallel$ events that are located near the EDR.

The proximity of $E_\parallel$ events near the EDR and the fluctuations in **B** suggest that these $E_\parallel$ events are associated with magnetic reconnection. The fluctuations in **B** suggest flux ropes or a tangled magnetic topology, for which there are several possible sources. One possibility is patchy reconnection, which can develop magnetic islands in two
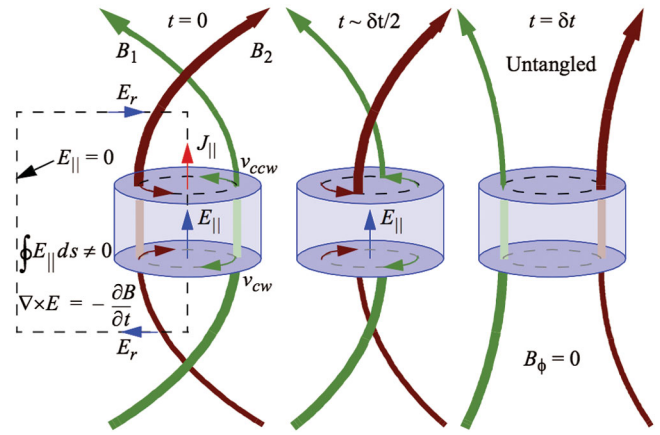


FIG. 4.   A three-dimensional visualization of how a $E_\parallel$ can untangle a flux rope.

dimensions or flux ropes if a guide field, even small, is present. Turbulence in the magnetosheath plasma, a common characteristic, may also cause patchy reconnection or tangled **B**. Alternatively, flux ropes or tangled **B** may be generated from turbulence resulting from the reconnection process or its outflow as has been observed in three-dimensional simulations [25,26].

The observations imply that the $E_\parallel$ events are dissipating currents that accompany **B** fluctuations. One hypothesis that we explore is that the unipolar $E_\parallel$ events represent secondary reconnection, e.g., [25], that is, strong guide-field reconnection within a magnetic flux rope or tangled **B**. Once developed, flux ropes or tangled **B** cannot necessarily propagate out of the diffusion region as jets, although they can propagate into the magnetosphere or magnetosheath. One possibility is that the flux rope does not propagate at all, which represents island formation in two dimensions. Another possibility, which we investigate here, is that small-scale flux ropes or tangled **B** can untangle or resolve if $E_\parallel$ develops.

The presence of strong, localized $E_\parallel$ on just one of the four MMS spacecraft implies that

$$\oint E_\parallel \cdot ds \neq 0. \tag{1}$$

The finite integral in Eq. (1) allows a magnetic field topology change [40,41]. Figure (4) shows a process of untangling magnetic fields in a cylindrical case. A localized $E_\parallel$ satisfying Eq. (1) and in the direction of a $J_\parallel$ can support dissipation of the azimuthal magnetic field ($B_\phi$) if $\boldsymbol{\nabla} \times \boldsymbol{E} \neq \boldsymbol{0}$. $E_\parallel$ can act as secondary reconnection only if the dissipated energy ($\boldsymbol{J} \cdot \boldsymbol{E}$) is sufficient to relax $B_\phi$. We can make a crude test from the observations, assuming cylindrical symmetry. The energy per unit length of the $B_\phi$ can be represented by

$$W_B \simeq \int_0^{R_B} \frac{B_\phi^2}{2\mu_o} 2\pi r dr = \frac{\langle B_\phi^2 \rangle}{2\mu_o} \pi R_B^2 \tag{2}$$

P H Y S I C A L  R E V I E W  L E T T E R S

where $R_B$ is a characteristic radius of the flux rope and $\langle B_\phi^2 \rangle$ is the integrated average of $B_\phi$. The energy dissipated per unit length can be expressed as

$$W_D \simeq \int \left[ \int_0^{R_{EJ}} \boldsymbol{E} \cdot \boldsymbol{J} 2\pi r dr \right] dt = \langle \boldsymbol{E} \cdot \boldsymbol{J} \rangle \pi R_{EJ}^2 \delta t \quad (3)$$

where $\delta t$ is the duration of the $E_\parallel$ event and $R_{EJ}$ is the extent of the dissipation region. Integrating $\langle \boldsymbol{J} \cdot \boldsymbol{E} \rangle \delta t$ [Fig. 1(i)] yields 0.5 nW s. Equations (2) and (3) then suggest that $B_\phi \sim 36$ nT can be dissipated if $R_B = R_{EJ}$. However, $B_\phi$ likely extends well past the region of $\boldsymbol{J} \cdot \boldsymbol{E} > 0$, so $R_B > R_{EJ}$. Setting $B_\phi \sim 5$ nT [from observed fluctuations in Fig. 1(d)] implies that $R_B \sim 3R_{EJ}$. The energy dissipation appears to be consistent with relaxation of $B_\phi$.

The scale sizes, $R_{EJ}$ and $R_B$, can be bounded. We can estimate that $R_{EJ}$ is less than $\sim 10$ km as only one spacecraft observes the $E_\parallel$ event. It is reasonable to assume a scale size larger than $\lambda_e$ ($\sim 2$ km). Another way to bound $R_B$ is to examine Faraday's law under the scenario in Fig. (4). However, Eq. (1) also must support radial electric fields ($E_r$) oppositely directed above and below the region of $E_\parallel$ to decrease magnetic helicity [40,41], reduce $J_\parallel$, and, in the end, untangle the fields. In other words,

$$\left| \oint E_\parallel \cdot ds \right| > \left| \oint E_r \cdot ds \right| \quad (4)$$

if there is to be reduction in $B_\phi$.

The finite value in Eq. (1) is balanced by $E_r$ (integrated) and by $-\partial B_\phi / \partial t$ (integrated over area). Using Faraday's law, we can approximate that $\varepsilon E_\parallel \delta t \sim R_B B_\phi$, where $\varepsilon < 1$ since $E_r$ contributes. Assigning $B_\phi = 5$ nT, and using the measured $E_\parallel \delta t$ [Fig. 1(j)], $R_B \sim \varepsilon 180$ km, implying that the $E_\parallel \delta t$ is more than sufficient to relax a small-scale flux rope.

While crude, these tests lend credence that the $E_\parallel$ structures may be associated with relaxation of turbulence near an EDR. Double layers have been reported from three-dimensional simulations of magnetic reconnection [25,26], particularly in low-$\beta$ plasmas [42]. Interestingly, most observed $E_\parallel$ events appear on the magnetosphere side of the reconnection, which generally has lower $\beta$ than the magnetosheath side.

*Conclusions.*—The MMS satellites have made unique observations of large-amplitude, near unipolar $E_\parallel$ events within several $\lambda_e$ of the EDR. During these $E_\parallel$ events, $V_i$ is decoupled from $V_e$ and $E$. $E_\parallel$ events are often observed on the magnetosphere side of the magnetopause, which has strong $\boldsymbol{B}$ and lower-density plasma than in the magnetosheath. $\boldsymbol{B}$ observations indicate fluctuations in $|\boldsymbol{B}|$ and/or in the perpendicular components, which is consistent with flux rope formation. The finite $E_\parallel$ is consistent with a possible change in magnetic field topology [40,41]. The measured dissipation ($\boldsymbol{J} \cdot \boldsymbol{E} \delta t$) is sufficient to dissipate $B_\phi$

of a flux rope. These observations suggest (1) magnetic reconnection is best described as a three-dimensional process that can be patchy and/or turbulent and results in tangled magnetic fields and (2) small-scale, secondary magnetic reconnection events can dissipate flux ropes that emerge from large-scale magnetic reconnection.

[1] J. L. Burch, T. E. Moore, R. B. Torbert, and B. L. Giles, Space Sci. Rev. **199**, 5 (2016).
[2] S. A. Fusilier, W. S. Lewis, C. Schiff, R. Ergun, J. L. Burch, S. M. Petrinec, and K. J. Trattner, W. S. Lewis, C. Schiff, R. Ergun, J. L. Burch, S. M. Petrinec, and K. J. Trattner, Space Sci. Rev. **199**, 77 (2016).
[3] G. B. Paschmann, B. U. Ö. Sonnerup, I. Papamastorakis, N. Sckopke, G. Haerendel, S. J. Bame, J. R. Asbridge, J. T. Gosling, C. T. Russell, and R. C. Elphic, Nature (London) **282**, 243 (1979).
[4] B. U. Ö. Sonnerup, G. Paschmann, I. Papamastorakis, N. Sckopke, G. Haerendel, S. J. Bame, J. R. Asbridge, J. T. Gosling, and C. T. Russell, J. Geophys. Res. **86**, 10049 (1981).
[5] M. Øieroset, T. D. Phan, M. Fujimoto, R. P. Lin, and R. P. Lepping, Nature (London) **412**, 414 (2001).
[6] F. S. Mozer, S. D. Bale, and T. D. Phan, Phys. Rev. Lett. **89**, 015002 (2002).
[7] P. Louarn et al., Geophys. Res. Lett. **31**, L19805 (2004).
[8] T. D. Phan, J. F. Drake, M. A. Shay, F. S. Mozer, and J. P. Eastwood, Phys. Rev. Lett. **99**, 255002 (2007).
[9] G. Paschmann, M. Øieroset, and T. Phan, Space Sci. Rev. **178**, 385 (2013).
[10] M. Hoshino and A. Nishida, J. Geophys. Res. **88**, 6926 (1983).
[11] D. Biskamp, E. Schwarz, and J. F. Drake, Phys. Plasmas **4**, 1002 (1997).
[12] M. A. Shay, J. F. Drake, R. E. Denton, and D. Biskamp, J. Geophys. Res. **103**, 9165 (1998).
[13] M. Hesse and D. Winske, J. Geophys. Res. **103**, 26479 (1998).
[14] J. Birn et al., J. Geophys. Res. **106**, 3715 (2001).
[15] P. L. Pritchett and F. V. Coroniti, J. Geophys. Res. **109**, A01220 (2004).
[16] J. F. Drake, M. Swisdak, H. Che, and M. A. Shay, Nature (London) **443**, 553 (2006).
[17] G. Lapenta, D. Krauss-Varban, H. Karimabadi, J. D. Huba, L. I. Rudakov, and P. Ricci, Geophys. Res. Lett. **33**, L10102 (2006).
[18] P. A. Cassak and M. A. Shay, Phys. Plasmas **14**, 102114 (2007).
[19] J. F. Drake, M. A. Shay, and M. Swisdak, Phys. Plasmas **15**, 042306 (2008).

[20] J. Egedal, A. Le, P. L. Pritchett, and W. Daughton, Phys. Plasmas **18**, 102901 (2011).

[21] M. Hesse, N. Aunai, D. Sibeck, and J. Birn, Geophys. Res. Lett. **41**, 8673 (2014).

[22] P. A. Cassak, R. N. Baylor, R. L. Fermo, M. T. Beidler, M. A. Shay, M. Swisdak, J. F. Drake, and H. Karimabadi, Phys. Plasmas **22**, 020705 (2015).

[23] J. Labelle and R. A. Treumann, Space Sci. Rev. **47**, 175 (1988).

[24] J. R. Shuster, L.-J. Chen, M. Hesse, M. R. Argall, W. Daughton, R. B. Torbert, and N. Bessho, Geophys. Res. Lett. **42**, 2586 (2015).

[25] G. Lapenta, S. Markidis, M. V. Goldman, and D. L. Newman, Nat. Phys. **11**, 690 (2015).

[26] W. Daughton, V. Roytershteyn, H. Karimabadi, L. Yin, B. J. Albright, B. Bergen, and K. J. Bowers, Nat. Phys. **7**, 539 (2011).

[27] J. L. Burch et al., Science (to be published).

[28] R. B. Torbert et al., Space Sci. Rev. **199**, 105 (2016).

[29] R. E. Ergun et al., Space Sci. Rev. **199**, 167 (2016).

[30] P.-A. Lindqvist et al., Space Sci. Rev. **199**, 137 (2016).

[31] C. T. Russell et al., Space Sci. Rev. **199**, 189 (2016).

[32] C. Pollock et al., Space Sci. Rev. **199**, 331 (2016).

[33] M. Øieroset, D. Sundkvist, C. C. Chaston, T. D. Phan, F. S. Mozer, J. P. McFadden, V. Angelopoulos, L. Andersson, and J. P. Eastwood, J. Geophys. Res. **119**, 6256 (2014).

[34] J. F. Drake, M. Swisdak, C. Cattell, M. A. Shay, B. N. Rogers, and A. Zeiler, Science **299**, 873 (2003).

[35] M. Øieroset et al., Phys. Rev. Lett. **107**, 165007 (2011).

[36] J. Zhong, J. Geophys. Res. **118**, 1904 (2013).

[37] L. Andersson, R. E. Ergun, D. L. Newman, J. P. McFadden, C. W. Carlson, and Y.-J. Su, Phys. Plasmas **9**, 3600 (2002).

[38] R. E. Ergun et al., Phys. Rev. Lett. **102**, 155002 (2009).

[39] D. L. Newman, M. V. Goldman, R. E. Ergun, and A. Mangeney, Phys. Rev. Lett. **87**, 255001 (2001).

[40] M. Hesse, T. Forbes, and J. Birn, Astrophys. J. **631**, 1227 (2005).

[41] M. Hesse and K. Schindler, J. Geophys. Res. **93**, 5559 (1988).

[42] J. Egedal, W. Daughton, A. Le, and A. L. Borg, Phys. Plasmas **22**, 101208 (2015).